Journal Pre-proof

Procedure to build a signal transfer set, independent of the target analytes, between a portable fluorimeter based on light-emitting diodes and a master fluorimeter

L. Rubio, S. Sanllorente, M.C. Ortiz, L.A. Sarabia

PII: S0003-2670(20)30141-0

DOI: https://doi.org/10.1016/j.aca.2020.01.072

Reference: ACA 237432

To appear in: *Analytica Chimica Acta*

Received Date: 21 October 2019

Revised Date: 27 January 2020

Accepted Date: 30 January 2020

Please cite this article as: L. Rubio, S. Sanllorente, M.C. Ortiz, L.A. Sarabia, Procedure to build a signal transfer set, independent of the target analytes, between a portable fluorimeter based on light-emitting diodes and a master fluorimeter, *Analytica Chimica Acta*, https://doi.org/10.1016/j.aca.2020.01.072.

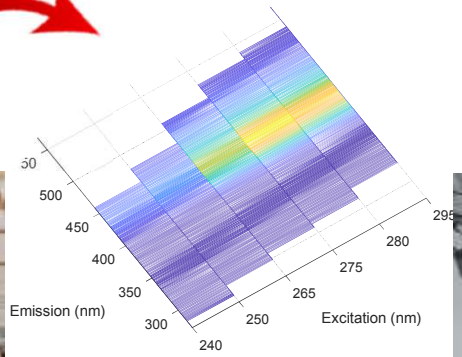

EEM Xenon lamp

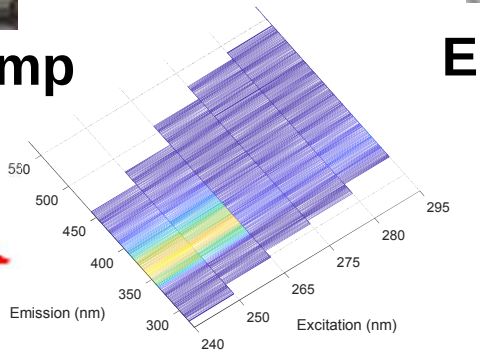

(e)

EEM with LEDs

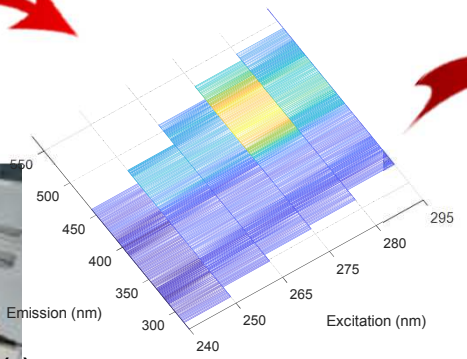

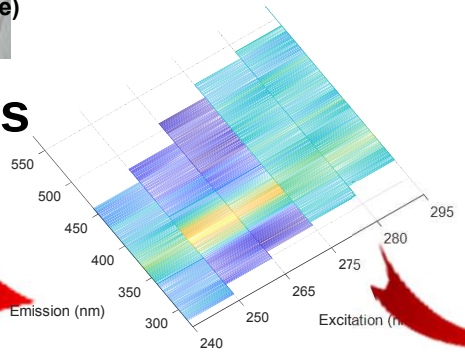

Transferred signals

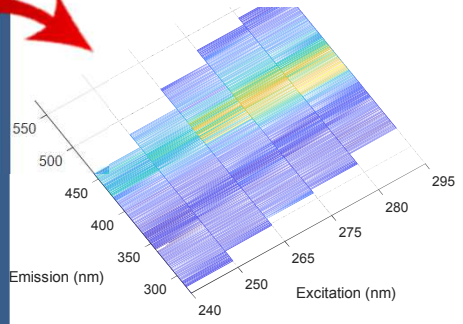

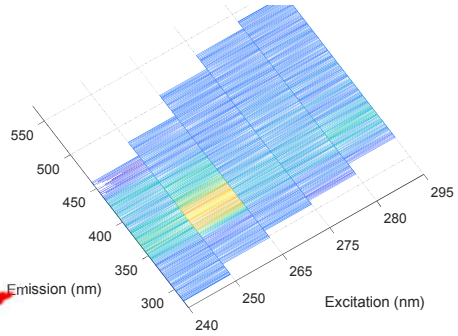

PROCEDURE TO BUILD A SIGNAL TRANSFER SET, INDEPENDENT OF THE TARGET ANALYTES, BETWEEN A PORTABLE FLUORIMETER BASED ON LIGHT-EMITTING DIODES AND A MASTER FLUORIMETER

L. Rubio[a], S. Sanllorente[a], M.C. Ortiz[a,1], L.A. Sarabia[b]

[a]*Department of Chemistry,* [b]*Department of Mathematics and Computation*

Faculty of Sciences, Universidad de Burgos

Plaza Misael Bañuelos s/n, 09001 Burgos (Spain)

Abbreviations[2]

ABSTRACT

The need of performing "*in situ*" analytical determinations together with the availability of high-power deep UV-LEDs have led to the use of fluorescence spectroscopy. However, it is necessary to register excitation-emission matrices (EEM) to obtain three-way data which can be decomposed using parallel factor analysis for enabling the unequivocal identification of the analytes. In this context, the feasibility of transferring EEM between a portable fluorimeter based on LEDs and a master fluorimeter based on a xenon source has been recently reported without losing analytical quality.

To build the transfer function, the signals of the same *N* samples must be recorded in the portable and in the master fluorimeter. In literature, these samples always contained the target analytes so the EEM signal transfer methodology is very limited in practice. Therefore, the challenge is to search for a set of samples whose EEM enable to perform the signal transfer without previously knowing the target analytes.

The aim of this work is the design of a procedure to build *N* mixtures of *P* fluorophores so the *N* EEM would be optimal for the signal transfer. Five criteria have been defined *a priori* to identify the quality of a transfer set made up of *N* EEM. Then, a procedure has been designed to obtain the *n* mixtures of the *P* fluorophores "in silico" using the Pareto front of the optimal solutions and a desirability function to choose the desired *N* EEM.

The procedure has been used to find five mixtures of the three chosen fluorophores for the signal transfer (coumarin 120, DL-Tyrosine and DL-Tryptophan) which are chemically different from the analytes of interest (enrofloxacin and flumequine) and are

[1] Corresponding author. Telephone number: 34-947-259571. *E-mail address*: mcortiz@ubu.es (M.C. Ortiz).

[2] Data cube of fluorescence intensities (CEEM), core consistency diagnostic (CORCONDIA), excitation-emission matrix (EEM), fluorescence intensity (IF), light-emitting diodes (LEDs), master fluorimeter (MF), parallel factor analysis (PARAFAC), portable fluorimeter (PF).

contained in a different matrix. These two analytes are antibiotics which have maximum residue limits set in the EU legislation in force.

The correlation coefficients between the experimental reference spectra and the PARAFAC spectral loadings of the data registered with the master fluorimeter were greater than or equal to 0.999 in all cases. On the other hand, the correlation coefficients obtained with the portable fluorimeter ranged from 0.900 to 0.950 once the procedure was applied to the two antibiotics. Therefore, the unequivocal identification of the analytes was ensured.

Keywords: Signal transfer; portable fluorimeter; excitation-emission fluorescence; PARAFAC; Pareto front; desirability function

1. Introduction

The IUPAC Technical Report [1] states that the focus of analytical chemistry and spectroscopic analysis is being on the "*in situ*" measurements which can be easily automated, particularly for the analysis of complex materials for fluorescence. This report considers the recording of excitation-emission matrices (EEM) together with parallel factor analysis (PARAFAC) as a promising tool due to the wide literature on the subject. In addition, this tool enables the identification and quantification of the target analytes in the presence of uncalibrated interferents (second-order property) [2]. However, the report also states that the EEM signal transfer between instruments is an open question whose importance is increasing due to the current tendency toward hosting open access online libraries of spectra that include EEM data [3,4].

From the point of view of instrumental portability, the use of LEDs has gained practical interest since the publication of Flaschka et al. [5], particularly in absorbance and fluorescence measurements as can be seen in reviews [6,7]. However, the research on the use of LEDs to generate EEM signals is limited [8,9,10,11]. In fact, EEM have not been used in [11].

The transfer of EEM between a portable fluorimeter based on light-emitting diodes (LEDs) and a conventional fluorescence spectrometer based on a xenon source has been reported for the first time in [10] with satisfactory results. The transfer function proposed in [12] was built in [10] with 5 EEM recorded in both instruments of the same samples which contained the same analytes as in the calibration and test samples. Then, for each pair of wavelengths (λ_{exc}, λ_{em}), a linear regression was built for the five fluorescence intensities recorded with the master fluorimeter *versus* the ones recorded with the portable instrument. The EEM signal was transferred between both fluorimeters with these regressions.

However, the transfer set used in refs. [10,12] contained the analytes that were going to be determined. This approach is enough for closed systems such as an industrial process or routine analyses in poultry drinking troughs. However, it is not general enough if samples that may contain different target analytes are measured "*in situ*" such as in the

analysis of pesticides, toxic residues of veterinary medicinal products or pollutants in environmental samples.

The aim of this work is the design of a procedure to build *N* mixtures of *P* fluorophores so the *N* EEM would be optimal for the signal transfer. The final purpose is to make the signal transfer independent from the analyte which is going to be detected outside the laboratory with the portable instrument and transfer it to the master instrument in the laboratory. The procedure has been applied to transfer the EEM signals using the calibrants: coumarin 120, DL-Tyrosine and DL-Tryptophan, which are chemically different from the analytes of interest of this work (enrofloxacin and flumequine). These fluoroquinolones have maximum residue limits set in the EU legislation in force [13] and are contained in a different matrix.

2. Material and methods

2.1. Chemicals

Enrofloxacin (CAS no. 93106-60-6), flumequine (CAS no. 42835-25-6), boric acid (CAS no. 10043-35-3; ≥ 99.8% purity) and phosphoric acid solution (85 wt. % in water) were purchased from Sigma-Aldrich (Steinheim, Germany). DL-Tryptophan (CAS no. 54-12-6; 98% purity), DL-Tyrosine (CAS no. 556-03-6; 99% purity) and 7-amino-4-methylcoumarin (coumarin 120, CAS no. 26093-31-2; 98% purity) were from Acros Organics (New Jersey, USA). Glacial acetic acid (CAS no. 64-19-7; HPLC grade) and sodium hydroxide (CAS no. 1310-73-2; pellets) were obtained from Panreac (Barcelona, Spain). Sodium acetate trihydrate (CAS no. 6131-90-4) was from VWR International, LLC (Radnor, Pennsylvania, USA). Ammonium hydroxide (CAS no. 1336-21-6) was obtained from Merck (Darmstad, Germany).

Deionised water was obtained by using the Milli-Q gradient A10 water purification system from Millipore (Bedford, MA, USA).

2.2. Standard solutions

The stock solution of enrofloxacin was prepared individually in 50 mM acetic acid aqueous solution at 1000 mg L^{-1}. Flumequine at 1000 mg L^{-1} was prepared in 1 M of ammonium hydroxide. Intermediate solutions at 100 mg L^{-1} were prepared daily by dilution with deionised water. The calibration and test samples were prepared adding the appropriate volume of the corresponding intermediate solutions and the sodium acetate/acetic acid buffer solution (0.02 M) at pH 4.

On the other hand, the individual stock solutions of coumarin 120, DL-Tyrosine and DL-Tryptophan at 35 mg L^{-1} and the corresponding samples that contained these compounds for the signal transfer set were prepared in Britton-Robinson buffer solution at pH 8. All the solutions were stored at 4 ºC protected from light.

2.3 Instrumental

Fluorescence measurements were performed at room temperature with two different instruments. The master fluorimeter was a PerkinElmer LS50B Luminescence Spectrometer (Waltham, MA, USA) equipped with a xenon discharge lamp. The EEM were recorded in the following ranges: excitation (240-295 nm, each 5 nm) and emission (270-550 nm, each 1 nm, for the samples measured in Section 3, and 270-600 nm, each 1 nm, for the rest of the cases). Excitation and emission monochromator slit widths were both set to 5 nm (10 nm in Section 3). The scan speed was 1500 nm min^{-1}.

The portable instrument was a spectrometer system for fluorescence (StellarNet Inc., Florida, USA) which consisted of an SL1-LED excitation source, a LED kit and a high-performance fiber optic spectrometer compact SILVER-Nova Super Range TE Cooled. Liquid samples were measured using the CUV-F liquid fluorescence. The emission spectra were recorded within the same range as in the master fluorimeter at the following excitation wavelengths (6 LEDs): 240 nm, 250 nm, 265 nm, 275 nm, 280 nm and 295 nm. The detector integration time was 10000 ms. The change of the LED was manual, so changes in the recorded fluorescent intensity might appear. To minimize this effect, all the emission spectra were registered with the same LED, then another LED was placed, and the emission spectra were recorded again.

A 10 mm quartz SUPRASIL® cell with cell volume of 3.5 mL by PerkinElmer (Waltham, MA, USA) was used in both instruments.

2.4 Software

The FL WinLab (PerkinElmer) and the SpectraWiz (StellarNet) software programs were used to record the fluorescent signals. The data were imported to MATLAB [14] using home-made functions to import data from both instruments, build the corresponding EEM at the same wavelengths and insert missing values into the matrix in the wavelengths that correspond to the Rayleigh effect [10]. The building of the transfer signal set (design, evaluation and optimization) was also performed using home-made software under MATLAB. The calculation of the Pareto front and its representation in parallel coordinates were done using the COOrdinates parallel plot and Pareto FROnt, COO-FRO, program [15]. PARAFAC decompositions were performed with the PLS_Toolbox 8.5.2 [16] used under MATLAB environment. The least squares regressions were built and validated with STATGRAPHICS Centurion XVII [17].

3. Methodology

For the first time, ref. [10] has shown with satisfactory results in the quantification and unequivocal identification that the transfer of the EEM recorded in a portable fluorimeter based on LEDs (PF) to a conventional fluorescence spectrometer based on a xenon source (MF) is possible. The transfer function proposed in [10] was built using 5

EEM recorded in both instruments, and a linear regression of the five fluorescence intensities registered with the MF *versus* the ones recorded with the PF was built for each (λ_{exc}, λ_{em}). The EEM signal from the PF to the MF was transferred point-by-point with these regressions.

The aim of this work is the design of a procedure to build *N* mixtures of *P* fluorophores so the *N* EEM matrices of dimension *I*×*J* could be arranged in a data array or cube of fluorescence intensities, CEEM = (IF_{nij}) of dimension *N*×*I*×*J*, which is optimal for the signal transfer.

3.1. Building of a set for the EEM signal transfer. Criteria for its evaluation

Once the CEEM arrays have been registered in both instruments, a regression for each pair of wavelengths (λ_{exc}, λ_{em}) is built. To obtain jointly the *I*×*J* regressions of the highest possible quality using only *N* mixtures of *P* calibrants, that is, *N* data for each of them, quantitative quality criteria that can be optimized are needed. The following five criteria associated with each CEEM were proposed for this purpose.

These criteria are described below qualitatively and in a formal language as a previous step of their optimization. A number is considered for each pair of wavelengths (λ_{exc}, λ_{em}) in each criterion, that is, *I*×*J* values which have to be managed together, except for criterion 1 since it is a count. The standard procedure is the use of a "*minimax*" or a "*maximin*" as appropriate. By way of example, when the minimum value of the *N* fluorescence intensities is considered, a "*minimax*" is used to manage all these *I*×*J* minimum values so the maximum value of all of them is calculated and this maximum is minimized. This is how criterion 4 has been built and optimized and the rest of the criteria are formalized analogously.

Criterion 1

This criterion is related to the idea that the signal transfer between instruments is better when the number of the regressions between the *N* intensities recorded in both instruments is higher. The signal transfer is also better if the number of pair of excitation and emission wavelengths (λ_i,λ_j) in which the *N* fluorescence intensities are below a threshold, *tr*, which could be considered only as noise, is lower.

$$crit_1 = card\left\{(i,j) \;/\; \max_{n\in\{1,2,\ldots,N\}}\left\{IF_{nij}\right\} < tr\right\} \quad (1)$$

Where "*card*" means the number of elements in the set. The $crit_1$ should be as low possible so the transfer could be performed in the widest region of the excitation and emission wavelengths.

Criterion 2.

Each of the regressions between the *N* intensities recorded in both instruments is more valid when the distribution of the *N* fluorescence intensity values, *IF*, is more uniform. The criterion 2 evaluates the uniformity of the *N* intensity values recorded at each pair

(λ_i,λ_j). This is calculated through the squared distance between the normalized vector of the fluorescence intensities ordered from least to greatest and the vector (1,2,…,*N*) also normalized. The greater this distance is, the less uniformly the fluorescence intensities are distributed in the *N* EEM. Therefore, $crit_2$ should be minimized to optimize the CEEM.

$$crit_2 = \max_{ij}\left\{\left(\frac{IF_{(1)ij}}{S_{ij}}-\frac{1}{S}\right)^2+\left(\frac{IF_{(2)ij}}{S_{ij}}-\frac{2}{S}\right)^2+\ldots+\left(\frac{IF_{(N)ij}}{S_{ij}}-\frac{N}{S}\right)^2\right\} \quad (2)$$

where $S_{ij}=\sum_{n=1}^{N} IF_{nij}$ and $S=\sum_{n=1}^{N}\mathrm{n}=(N+1)\times N/2$. The subscript (*n*)*ij* means that the *N* values of *IF* in the pair of excitation and emission wavelengths (λ_i,λ_j) have been arranged in increasing order.

Criterion 3.

It is clear that the regression in each pair of wavelengths (λ_i, λ_j) is more stable when the range of the *N* fluorescence intensity values is greater. This is the reason why each CEEM is evaluated by the minimum range of the *N* intensities. This criterion will be maximized.

$$crit_3 = \min_{ij}\left\{IF_{(N)ij}-IF_{(1)ij}\right\} \quad (3)$$

The subscript (*n*)*ij* means that the *IF* values are arranged in increasing order for each (*i*,*j*) as in Eq. (2).

Criterion 4.

Evaluation of the lowest fluorescence intensity, $IF_{(1)ij}$, in each pair of excitation and emission wavelengths. The most adequate CEEM will be obtained when the highest value of the pair (λ_i,λ_j) is minimized, that is, if $crit_4$ is minimized.

$$crit_4 = \max_{ij}\left\{IF_{(1)ij}\right\} \quad (4)$$

where the subscript (*1*)*ij* has the same meaning as in Eq. (3).

Criterion 5.

The regression is better when the maximum value of the fluorescence intensities, $IF_{(N)ij}$, is higher. When all the pair of excitation and emission wavelengths are considered, the minimum value of these maximum is crit5, which is defined in Eq. (5). In this case, $crit_5$ should be maximized to obtain a CEEM more adequate for the signal transfer.

$$crit_5 = \min_{ij}\left\{IF_{(N)ij}\right\} \quad (5)$$

where the subscript $(N)ij$ has the same meaning as in Eq. (3).

To sum up, the defined criteria expect to guarantee *a priori* the highest possible number of the regressions "intensity recorded in the MF *versus* the one obtained in the PF" (criterion 1) as well as their quality. This means that the values of the fluorescence intensity recorded in the MF should have the highest possible range, the maximum uniformity in that range and that their minimum and maximum values should be the most extreme ones. These properties are quite independent of each other, so they are considered together in the design process of the CEEM and its subsequent optimization.

The criteria proposed in this section are adapted to an EEM signal transfer using univariate regressions in each pair of excitation and emission wavelengths, (λ_i,λ_j). If the procedure to transfer the signals is modified, new criteria to optimize that transfer would need to be defined. By way of example, if a rectangular area is considered instead of a pair of wavelengths, a multivariate/multi-response problem appears which should be modelled by PLSR. This increases the complexity of the model of the transfer and its building, but it would be more robust and smoother. The adaptation of the criteria 2-5 to this new structure will be the subject of future research.

3.2. Procedure to design CEEM cubes in silico

The steps of the procedure are the following ones:

(i) Build a PARAFAC model for each of the *P* fluorophores. To do this, *M* standard samples are prepared for each of the *P* calibrants at concentrations within the ranges $R_1,\ldots,R_P$. As a consequence, a CEEM is obtained of dimension $M\times I\times J$ which corresponds to the number of samples, emission and excitation wavelengths, respectively.

(ii) A normalized EEM_p of each fluorophore, p = 1,..,*P*, is built with the loadings of the excitation and emission profiles of each PARAFAC model after its unequivocal identification. In addition, *P* calibration functions are also built with the least-squares regressions "sample loadings *versus* true concentration". In this way, the EEM_p signal of each calibrant is characterized as well as its sensitivity when the concentration increases.

(iii) *N* vectors (c_{1n}, c_{2n},… c_{Pn}) n=1,2,…,*N* of dimension *P*, which represent the concentrations of the *P* calibrants, are chosen in the ranges of each of them, $R_1,\ldots,R_P$ respectively. When the corresponding calibration functions are applied, *N* vectors of loadings (l_{1n}, l_{2n}, ….l_{Pn}) n =1,2,…,*N* in the sample profile are obtained. Finally, the $EEM_n = \sum_{p=1}^{P} l_{pn} EEM_p$ n = 1,…, *N* is built for each of the *N* mixtures of the *P* calibrants.

Once they are concatenated, a CEEM is obtained in which the five criteria described in Section 3.1 are evaluated. In this way, each CEEM is identified by the concentrations of the *P* calibrants in the *N* mixtures (*P*×*N* values) and characterized by the values of the five criteria.

3.3. Optimization of the CEEM cubes in silico

The problem is to find the *P*×*N* concentration vectors with coordinates belonging to $(R_1\times\ldots\times R_P)^N$, named as $\mathfrak{D}^N$, that simultaneously minimize the criteria 1, 2 and 4 and maximize the criteria 3 and 5 of section 3.1.

A grid is built in the region $\mathfrak{D}^N$ and the Monte Carlo method is applied in it [18]. Specifically, a set of vectors have been randomly generated, with uniform distribution, and the 5 criteria have been evaluated in the corresponding CEEMs generated with the procedure described in Section 3.2.

A direct comparison is not possible to decide which CEEM is better according to the five criteria since there is not an order between vectors similar to the real numbers. The concept of dominated CEEM is used as an alternative. The Pareto front of the CEEM set is made up of the non-dominated arrays. In practice, it is only useful to explore the Pareto front [19,20] since any other CEEM would be worse in some of the five criteria. The procedure is repeated *k* times and the CEEM of the *k* Pareto fronts are arranged to obtain a final optimal non-dominated Pareto front.

The proposed methodology in this section enables to study the effect of changing and/or adding calibrants. A PARAFAC calibration for each of the calibrants is needed to obtain their EEM matrix and their analytical sensitivity. Then, new EEM cubes are built with more or a smaller number of mixtures. Finally, the five criteria and a new Pareto front will be calculated with these CEEM. Therefore, a different Pareto front is obtained for each case of *P* calibrants and *N* mixtures, and the comparison between them would enable the evaluation of the degree of improvement and on which criteria.

4. Results and discussion

4.1. Building of the optimal array for the signal transfer

In this work, the calibrants were three, *P*=3, and the concentration ranges (R_1,R_2 and R_3) for coumarin 120, DL-Tyrosine and DL-Tryptophan were [0 - 35], [0 - 2720] and [0 - 300] µg L^{-1}, respectively. The concentrations were 0, 2, 5, 10, 15, 20 and 35 µg L^{-1} for coumarin 120; 0, 175, 680, 1360, 2040, 2500 and 2720 µg L^{-1} for DL-Tyrosine; and 0, 20, 60, 120, 180, 240 and 300 µg L^{-1} for DL-Tryptophan. Therefore, to apply step (i) of section 3.2, *M* = 7 in the three cases so the dimension of the cube was 7×278×12, which corresponds to the number of samples, emission and excitation wavelengths, respectively.

The characteristics of the PARAFAC models and of the calibration lines are included in Tables 1 and 2, respectively. The CORCONDIA indexes indicated trilinearity and the coefficient of determination, R^2, was greater than 99.9% in the three calibrations.

Table 1 Characteristics of the PARAFAC models obtained for each fluorophore in the master fluorimeter.

	Coumarin 120	DL-Tyrosine	DL-Tryptophan
Constraints	Non-negativity*	Non-negativity*	Non-negativity*
Number of factors	2	2	2
CORCONDIA	87	100	100
Split-half analysis**	95.5	99.5	99.2
Total variance Captured (% **X**)	91.27	98.74	95.86
Variance Captured (% Model)			
First factor	98.66	99.33	99.75
Second factor	1.34	0.67	0.25
Identification			
First factor	Coumarin 120	DL-Tyrosine	DL-Tryptophan
Second factor	Background	Background	Background

*In the three modes

**Similarity measure of splits and overall model in percent

Table 2 Parameters of the calibration line for each fluorophore using the PARAFAC sample loading *versus* true concentration.

	Coumarin 120	DL-Tyrosine	DL-Tryptophan
Intercept	250.87	145.75	143.79
Slope	308.24	3.90	52.14
Significance test (p-value)	$< 10^{-5}$	$< 10^{-5}$	$< 10^{-5}$
R^2 (%)	99.95	99.92	99.90
s_{yx}	96.83	136.00	202.82

R^2: Coefficient of determination. s_{yx}: Residual standard deviation

Fig. 1 shows the EEM_p (p = 1,2,3) matrices for the three fluorophores (Coumarin 120, DL-Tyrosine and DL-Tryptophan). These EEM_p matrices are the tensor product of the normalized loadings of the excitation and emission profiles of each PARAFAC model (see step (ii) of section 3.2).

For the building of the data arrays with N=5 mixtures of the three EEM_p (step (iii) of section 3.2), the concentration values in $\mathcal{D}$ = [2-35]×[175-2720]×[20-300] were considered, which is the domain (in µg L^{-1}) for the concentrations of coumarin 120, DL-Tyrosine and DL-Tryptophan. This domain is the same already considered except for the zero concentration of each of them to obtain ternary mixtures. In addition, the excitation wavelengths should be the same in the MF and PF to carry out the signal transfer. Therefore, the six excitation wavelengths corresponding to the LEDs were chosen so the EEM_p (p =1,2,3) matrices are of dimension 278×6.

The signals corresponding to the mixtures, $EEM_n = \sum_{p=1}^{3} l_{np} EEM_p$ n=1,2,…,5, were built with these EEM_p matrices. Once they were concatenated, a CEEM was obtained in which the five criteria described in Section 3.1 were evaluated. The CEEM with computed fluorescence intensities greater than 900 was rejected to avoid measuring samples which can saturate the detector of the MF used.

As a consequence of the building of the CEEM described in the previous paragraph, each of them contains 5 EEM matrices that depend on three concentrations selected in the domain $\mathcal{D}$ = [2-35]×[175-2720]×[20-300], that is, it is a function of 15 values. When the optimization procedure described in section 3.3 was applied, a discretization was carried out in the search region from µg L^{-1} to µg L^{-1} and 1000 points of the grid were chosen to obtain the Pareto front of the non-dominated solutions. This procedure was repeated 10 times and 10 Pareto fronts made up of 108, 87, 67, 106, 82, 79, 60, 86, 99 and 96 CEEM were obtained and arranged in a new set of 855 different CEEM, whose Pareto front is made up of 201 optimal non-dominated CEEM. The function "FPareto.m" in Annex A of ref. [15], which is written in MATLAB, was used to obtain the Pareto front in the software.

The value of the criteria for these 201 solutions is displayed in Fig. 2a through the parallel coordinates plot [21,22] which shows the five criteria in five vertical axes. Each polygonal joins the five values of *crit*i, i=1,..,5 which correspond to a CEEM of the Pareto front. In order to improve the visibility of the lines, the range of each criterion has been transformed, so it is [0,1] for all the criteria. However, the minimum and maximum values of each criterion have been written at the end of the parallel axes. Fig. 2a has been obtained using the "CPFP script" of Annex A of ref. [15].

The 10000 CEEM generated provide values of the five criteria in wider ranges than the ones of the Pareto front shown in Fig. 2a. These values vary between 93 and 312, 0.033 and 1.340, 0.315 and 8.823, 96.148 and 817.208 10.00 and 10.34 for each criterion, respectively, so the Monte Carlo method has obtained a reduction of a factor between 40.61 and 3.35 in the values of the criteria 1, 2 and 4. On the other hand, an increase in a factor of 28.00 and 1.03 has been obtained for the criteria 3 and 5.

Fig. 2a shows the conflict between the criteria. By way of example, the lowest values of $crit_1$ are obtained with CEEM that do not have the lowest values of $crit_2$. To reach a compromise solution, the desirability function defined in [23] has been used, which is used widespread in the experimental multicriteria optimization [24]. The idea is to convert the values of the criteria using functions with values between 0 and 1 that consider which are the admissible values and which not.

The individual desirability function d_i, i=1,2,4, for the criteria to minimize ($crit_1$, $crit_2$ and $crit_4$) is:

$$\begin{aligned} &d_i(crit_i) = 1 \text{ if } crit_i \text{ is below the 10th percentile} \\ &d_i(crit_i) = 0 \text{ if } crit_i \text{ is above the 75th percentile} \\ &d_i(crit_i) \text{ linear between both values} \end{aligned} \quad (6)$$

The individual desirability function d_i, i=3,5, for the criteria to maximize ($crit_3$ and $crit_5$) is:

$d_i(crit_i) = 1$ if $crit_i$ is above the 90th percentile
$d_i(crit_i) = 0$ if $crit_i$ is below the 25th percentile (7)
$d_i(crit_i)$ linear between both values

The use of the percentiles of the criteria and not their target values in the individual desirability functions has the advantage that scale and range effects, which are quite different from one criterion to another, are avoided.

Finally, the global desirability function, *D*, assigns the weighted geometric mean of functions d_i i=1,2,..,5 to each CEEM. The weights show the importance of each of the criteria to achieve a signal transfer of enough quality. It is considered that having a greater number of regressions with fluorescence intensity above the threshold value and that the values are uniformly distributed in the range are more influential characteristics than the range. In addition, the range is a more influential characteristic than the maximum and minimum values.

$$D(crit_1, crit_2, \ldots, crit_5) = d_1^{3/10}\ d_2^{3/10}\ d_3^{2/10}\ d_4^{1/10}\ d_5^{1/10} \quad (8)$$

The value of function *D* for each of the 201 CEEM of the Pareto front is shown in Fig. 2b in which the maximum has been marked. The values of the criteria for this $CEEM_{Dmax}$ are 98, 0.0634, 7.0221, 212.78 and 10.0939, which are marked in red on Fig. 2a. When these values are compared with the minimum and maximum value of each criterion in the Pareto front of Fig. 2a, it is clear that a compromise has been considered.

Fig. 3 shows the five EEM that made up $CEEM_{Dmax}$ which correspond to the mixtures of Table 3.

Table 3 Concentration, in µg L^{-1}, of the three calibrants for each EEM of $CEEM_{Dmax}$

EEM	coumarin 120	DL-Tyrosine	DL-Tryptophan
1	22	1599	185
2	32	1913	74
3	7	1146	187
4	34	2097	228
5	12	312	22

4.2. Experimental results in the determination of the target analytes after the transference has been applied

The mixtures of coumarin 120, DL-Tyrosine and DL-Tryptophan were prepared at the concentrations of Table 3. These samples were measured in both fluorimeters at the conditions described in Section 2.3. Then, the data were imported and the transfer function was built between the EEM signals of the PF and the ones of the MF as described in ref. [10].

The signal transfer was applied to EEM corresponding to the measurement of samples containing enrofloxacin, flumequine and mixtures of both of them (see Table 4) with the aim of identifying both analytes which have been determined in the PF and the signal has been transferred to the MF.

Table 4 Concentration of the samples used for the identification

			Binary mixtures	
	ENR ($\mu g\ L^{-1}$)	FLU ($\mu g\ L^{-1}$)	ENR ($\mu g\ L^{-1}$)	FLU ($\mu g\ L^{-1}$)
Set1				
1	0	0	0	0
2	50	100	50	0
3	100	200	100	0
4	200	300	150	0
5	75	400	0	150
6	125	500	50	150
7	175	600	100	150
8			150	150
9			0	300
10			50	300
11			100	300
12			150	300
13			0	450
14			50	450
15			100	450
16			150	450
Set2				
1	150	250	75	225
2	100	530	60	170
3	175	375	85	380
4	65	425	125	275
5	130	310	110	400

ENR enrofloxacin, FLU flumequine

Fig. 4 graphically shows the differences between the EEM corresponding to the same sample of enrofloxacin or flumequine registered with the MF (Fig. 4a and Fig. 4d) or with the PF (Fig. 4b and Fig. 4e). The effect of the transfer is also verified by modifying the EEM of the PF to make it more similar to the one recorded with the MF.

These two previous EEM, registered with the MF, were used to obtain the emission reference spectrum, which was taken at the excitation wavelength of 275 nm for enrofloxacin and 240 nm for flumequine, whereas the excitation reference spectrum was considered at the emission wavelength of 437 nm for enrofloxacin and 356 nm for flumequine. A PARAFAC model was built with the arrays that contained the transferred EEM of Set1, Set2 and Set1∪ Set2 (TR_{S1}, TR_{S2} and TR_{S1US2}, respectively) and a spectral loading of the excitation and emission profile was obtained. Then, the correlation coefficient with the reference spectra was evaluated.

The correlation coefficients of the PARAFAC spectral loadings of Set1 obtained with the samples recorded in the MF (MF_{S1}) have also been calculated for comparative purposes. This is the greatest possible value of the correlation.

The results are shown in Table 5. From the 24 cases of transferred EEM, 7 of them had correlations with the reference spectra between 0.9 and 0.95, whereas 15 of them were greater than 0.95. Therefore, the unequivocal identification of flumequine and enrofloxacin was possible using the signals registered in the PF and transferred to the MF.

In all cases, the correlation coefficient between the reference spectra and the spectral loadings of the data recorded with the MF were equal or greater than 0.999.

Table 5 Correlation coefficients between the PARAFAC loadings and the excitation and emission reference spectra

	Spectral loadings of the specified array			
	MF_{S1}	TR_{S1}	TR_{S2}	$TR_{S1 \cup S2}$
Samples of enrofloxacin, column 2 of Table 4				
EXRS[a]	0.9990	0.7994	0.9544	0.8896
EMRS[b]	0.9998	0.9885	0.9883	0.9886
Samples of flumequine, column 3 of Table 4				
EXRS[a]	0.9996	0.9661	0.9681	0.9675
EMRS[b]	0.9995	0.9536	0.9454	0.9503
Enrofloxacin in the binary mixtures, columns 4 and 5 of Table 4				
EXRS[a]	0.9993	0.9085	0.9085	0.9237
EMRS[b]	0.9996	0.9844	0.9844	0.9851
Flumequine in the binary mixtures, columns 4 and 5 of Table 4				
EXRS[a]	0.9998	0.9606	0.9606	0.9803
EMRS[b]	0.9990	0.9092	0.9092	0.9029

[a] EXRS stands for Excitation Reference Spectrum
[b] EMRS stands for Emission Reference Spectrum

5. Conclusions

This is the first time that the problem of building an array for the signal transfer using N EEM matrices obtained by the recording of mixtures of P fluorophores has been addressed. The designed procedure to make experiments "*in silico*" enabled the selection of optimal mixtures for the signal transfer with experimental EEM using chemically different compounds from the target analytes and in a different media. This is an essential step to perform fluorescence measurements with a portable instrument in a regular framework.

Therefore, some quality characteristics of the cube have to be defined as well as the information needed to build EEM cubes *in silico*: (i) make completely independent the selection of the mixtures of the calibrants of the analytes to be measured, and (ii)

explicitly consider the analytical sensitivity of each compound and its EEM by PARAFAC.

The new proposed procedure enabled the unequivocal identification of the analytes with measurements carried out on the portable LEDs based instrument.

The proposed methodology will have to be evaluated in other problems of transfer of EEM signals.

CONFLICT OF INTEREST

The authors declare no competing financial interest.

Acknowledgements

The authors thank the financial support provided by Spanish MINECO (AEI/FEDER, UE) through project CTQ2017-88894-R and by Junta de Castilla y León through project BU012P17 (all co-financed with European FEDER funds).

References

[1] A.G. Ryder, C.A. Stedmon, N. Harrit, R. Bro, Calibration, standardization, and quantitative analysis of multidimensional fluorescence (MDF) measurements on complex mixtures (IUPAC Technical Report), Pure Appl. Chem. 89 (2017) 1849-1870.

[2] R. Bro, PARAFAC. Tutorial and applications, Chemometr. Intell. Lab. 38 (1997) 149-171.

[3] K.R. Murphy, C.A. Stedmon, P. Wenig, R. Bro, OpenFluor– an online spectral library of auto-fluorescence by organic compounds in the environment, Anal. Methods 6 (2014) 658-661.

[4] H. Hassoun, T. Lamhasni, S. Foudeil, A. El Bakkali, S.A. Lyazidi, M. Haddad, M. Choukrad, M. Hnach, Total Fluorescence Fingerprinting of Pesticides: A Reliable Approach for Continuous Monitoring of Soils and Waters, J. Fluoresc. 27 (2017) 1633-1642.

[5] H. Flaschka, C. McKeithan, R. Barnes, Light Emitting Diodes and Phototransistors in Photometric Modules, Anal. Lett. 6 (1973) 585-594.

[6] M. Macka, T. Piasecki, P.K. Dasgupta, Light-Emitting Diodes for Analytical Chemistry, Annu. Rev. Anal. Chem. 7 (2014) 183-207.

[7] D.A. Bui, P.C. Hauser, Analytical devices based on light-emitting diodes - a review of the state-of-the-art, Anal. Chim. Acta 853 (2015) 46-58.

[8] S.J. Hart, R.D. JiJi, Light emitting diode excitation emission matrix fluorescence Spectroscopy, Analyst 127 (2002) 1693-1699.

[9] S. Obeidat, B. Bai, G.D. Rayson, D.M. Anderson, A.D. Puscheck, S.Y. Landau, T. Glasser, A Multi-Source Portable Light Emitting Diode Spectrofluorometer, Appl. Spectrosc. 62 (2008) 327-332.

[10] S. Sanllorente, L. Rubio, M.C. Ortiz, L.A. Sarabia, Signal transfer with excitation-emission matrices between a portable fluorimeter based on light-emitting diodes and a master fluorimeter, Sens. Actuators, B 285 (2019) 240-247.

[11] M.T. Taschuk, Q. Wang, S. Drake, A. Ewanchuk, M. Gupta, M. Alostaz, A. Ulrich, D. Sego, Y.Y. Tsui, Portable naphthenic acids sensor for oil sands applications, Proceedings of the Second International Oil Sands Tailings Conference, Edmonton, Alberta.

[12] J. Thygesen, F. van den Berg, Calibration transfer for excitation–emission fluorescence measurements, Anal. Chim. Acta 705 (2011) 81-87.

[13] Commission Regulation (EU) No 37/2010 of 22 December 2009, Off. J. Eur. Union, L 15 (2010) 1-72.

[14] MATLAB version 9.4.0.813654 (R2018a), The Mathworks, Inc., Natick, MA, USA, 2018.

[15] M.M. Arce, S. Sanllorente, M.C. Ortiz, L.A. Sarabia, Easy-to-use procedure to optimise a chromatographic method. Application in the determination of bisphenol-A and phenol in toys by means of liquid chromatography with fluorescence detection, J. Chromatogr. A 1534 (2018) 93-100.

[16] B.M. Wise, N.B. Gallagher, R. Bro, J.M. Shaver, W. Windig, R.S. Koch, PLS Toolbox 8.6.2, Eigenvector Research Inc., Manson, WA, USA, 2018.

[17] STATGRAPHICS Centurion 18 Version 18.1.11 (64 bit), Statpoint Technologies, Inc., Warrenton, VA, USA, 2018.

[18] J.S. Liu, Montecarlo Strategies in Scientific Computing, Springer-Verlag, New York Berlin Heidelberg, 2003.

[19] M.S. Sánchez, M.C. Ortiz, L.A. Sarabia, R. Lletí, On Pareto-optimal fronts for deciding about sensitivity and specificity in class-modelling problems, Anal. Chim. Acta 544 (2005) 236-245.

[20] C. Reguera, M.S. Sánchez, M.C. Ortiz, L.A. Sarabia, Pareto-optimal front as a tool to study the behaviour of experimental factors in multi-response analytical procedures, Anal. Chim. Acta 624 (2008) 210-222.

[21] A. Inselberg, Parallel Coordinates: Visual Multidimensional Geometry and Its Applications, Springer, Dordrecht, Heidelbeg, 2009.

[22] M.C. Ortiz, L.A. Sarabia, M.S. Sánchez, D. Arroyo, Improving the visualization of the Pareto-optimal front for the multi-response optimization of chromatographic determinations, Anal. Chim. Acta 687 (2011) 129-136.

[23] G. Derringer, R. Suich, Simultaneous optimization of several response variables, J. Qual. Technol. 12 (1980) 214-219.

[24] L.A. Sarabia, M.C. Ortiz, Response surface methodology, in: Comprehensive Chemometrics: Chemical and Biochemical Data Analysis, (eds.), Elsevier, Amsterdam, Holland, 2009, pp. 378–382.

FIGURE CAPTIONS

Fig. 1 Normalized EEM landscape of a) Coumarin 120, b) DL-Tyrosine, c) DL-Tryptophan obtained through the PARAFAC model.

Fig. 2 a) Parallel coordinates plot of the 201 optimal arrays of the Pareto front for each criterion; the red line is the best global desirability solution found, b) Values of the global desirability function for each one of the 201 optimal arrays of the Pareto front. The optimal solution is represented by a red cross.

Fig. 3 EEM landscapes of the five optimal mixtures, a) 1, b) 2, c) 3, d) 4, e) 5, for the signal transfer.

Fig. 4 Contour plots of: (a-c) a test sample containing 130 µg L^{-1} of enrofloxacin and (d-f) a test sample containing 375 µg L^{-1} of flumequine. EEM recorded: a) and d) in the master fluorimeter, b) and e) in the portable fluorimeter, c) and f) transferred from the portable fluorimeter to the master one.

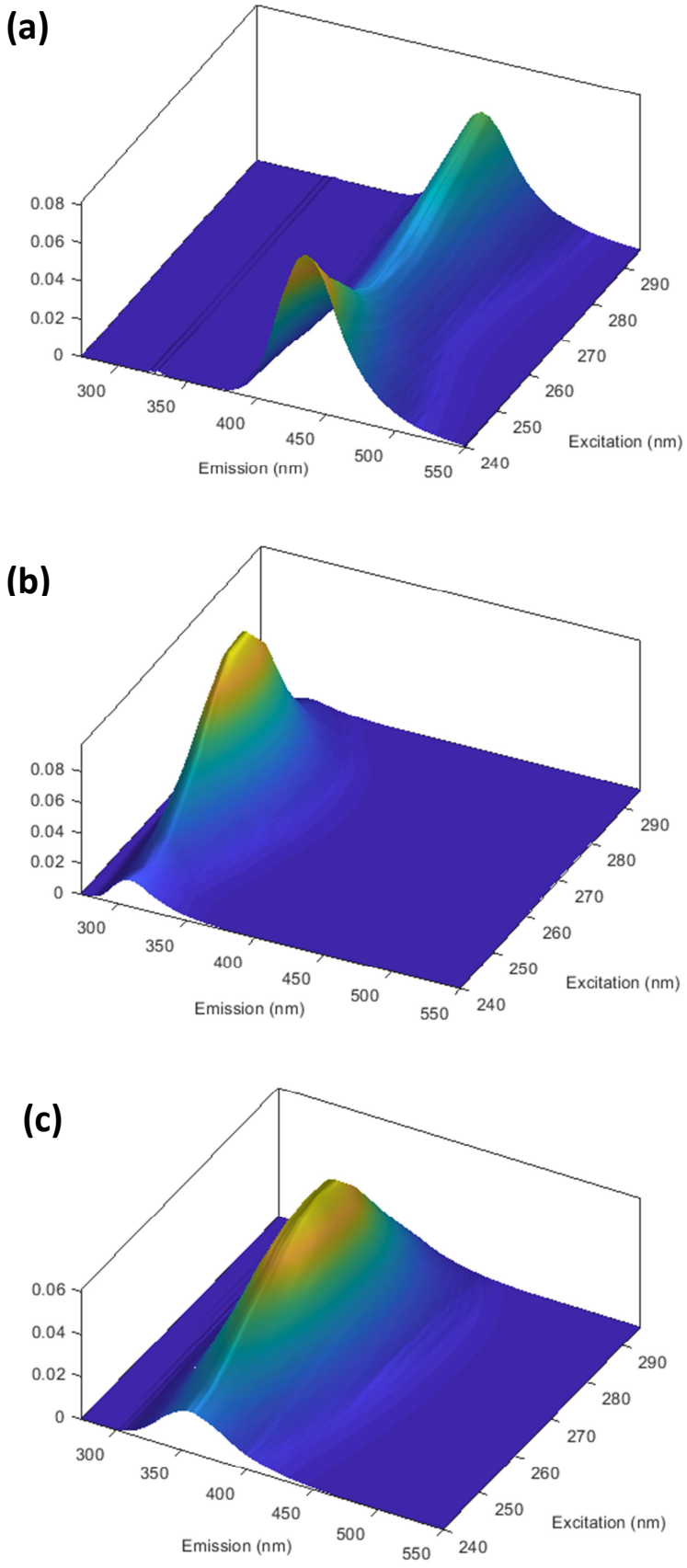
(a)
0.08
0.06
0.04
0.02
0
300
350
400
450
500
550
Emission (nm)
240
250
260
270
280
290
Excitation (nm)
(b)
0.08
0.06
0.04
0.02
0
300
350
400
450
500
550
Emission (nm)
240
250
260
270
280
290
Excitation (nm)
(c)
0.06
0.04
0.02
0
300
350
400
450
500
550
Emission (nm)
240
250
260
270
280
290
Excitation (nm)

Fig. 1

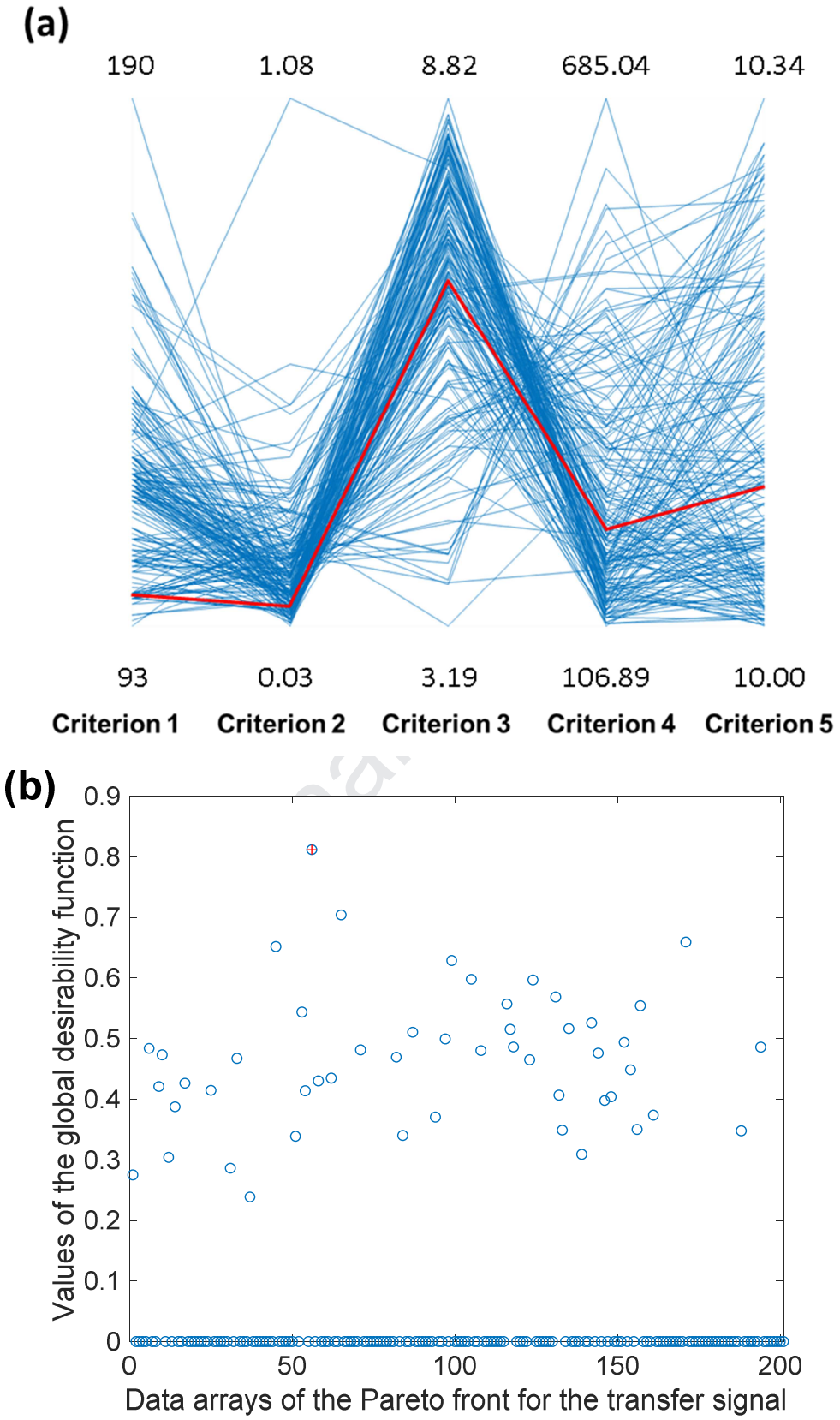
(a)
190
1.08
8.82
685.04
10.34
93
0.03
3.19
106.89
10.00
Criterion 1
Criterion 2
Criterion 3
Criterion 4
Criterion 5
(b)
Values of the global desirability function
0
0.1
0.2
0.3
0.4
0.5
0.6
0.7
0.8
0.9
0
50
100
150
200
Data arrays of the Pareto front for the transfer signal

Fig. 2

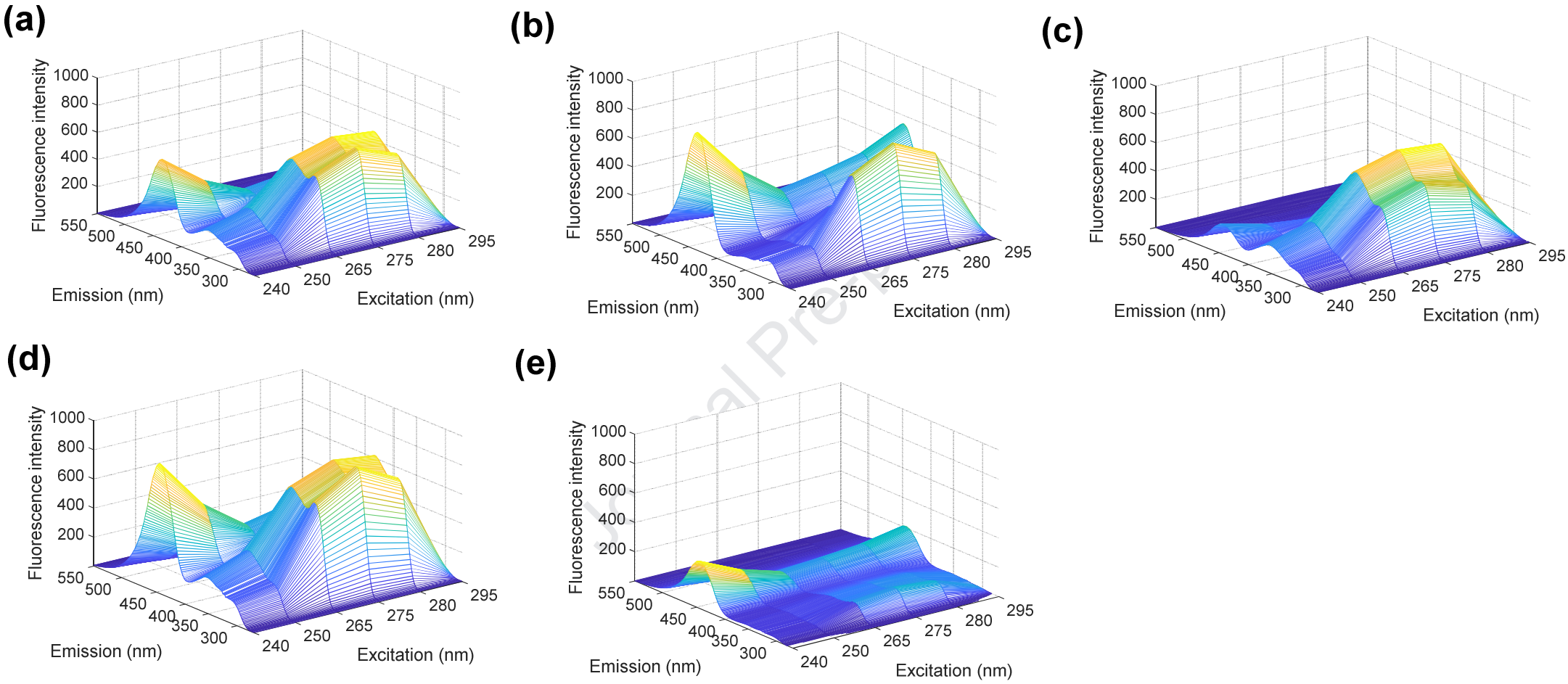
(a)
(b)
(c)
(d)
(e)
Fluorescence intensity
1000
800
600
400
200
Emission (nm)
550
500
450
400
350
300
Excitation (nm)
240
250
265
275
280
295

Fig. 3

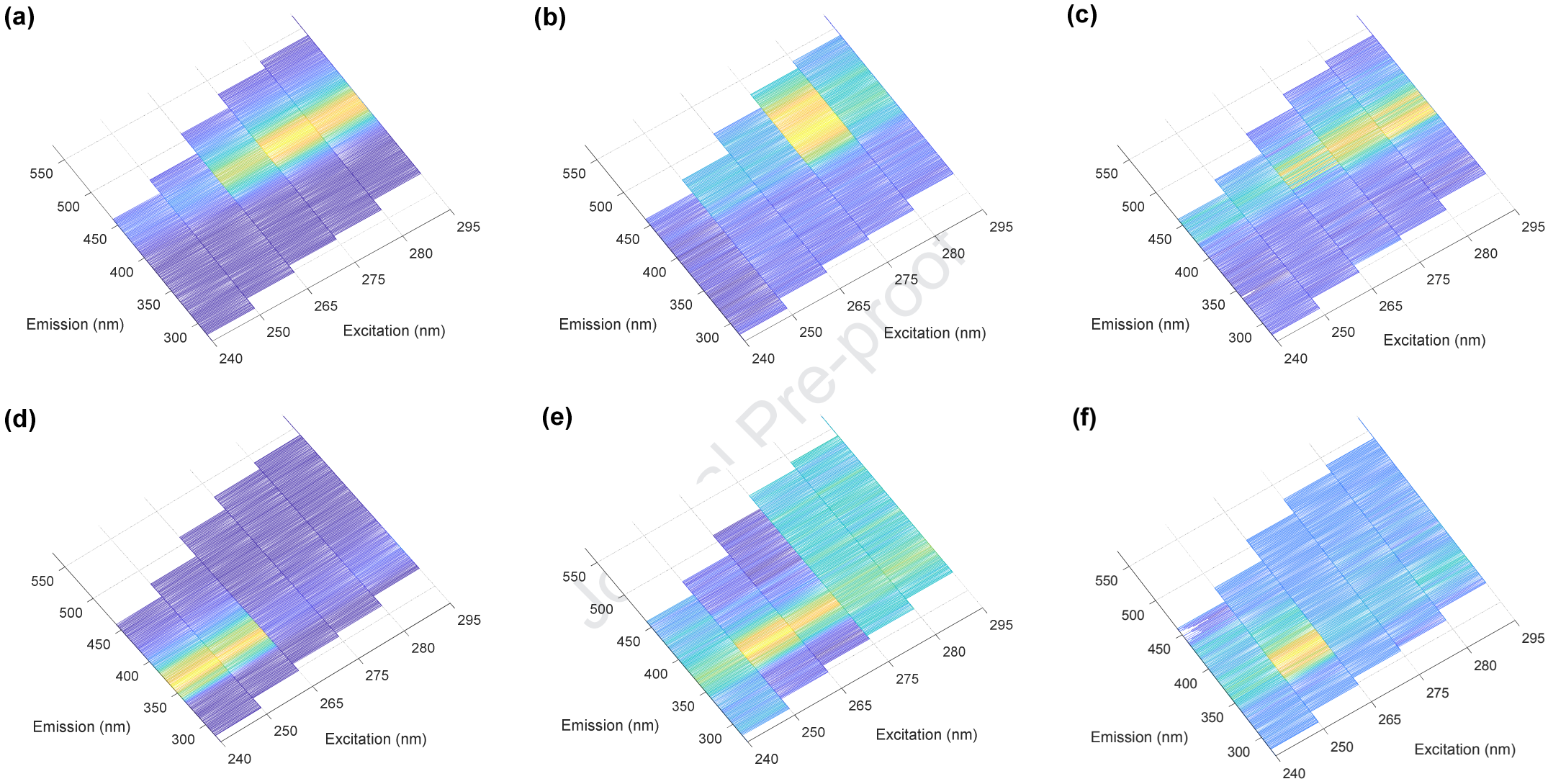

Fig. 4

HIGHLIGHTS

EEM transfer between fluorimeters with LEDs and a xenon lamp as excitation sources

The procedure enabled the selection of optimal mixtures for the EEM signal transfer

The Pareto front and a desirability function were used to select the optimal EEM

The calibrants used in the signal transfer are chemically different from the analytes

A new procedure enabled the unequivocal identification of enrofloxacin and flumequine

Credit Author Statement:

L. Rubio: Investigation, Analytical Methodology Writing - Original Draft, Supervision

S. Sanllorente: Investigation, Analytical Methodology, Supervision, Writing - Review & Editing

L.A. Sarabia Conceptualization, Methodology,Formal analysis, Software, Supervision, Writing - Review & Editing

M.C. Ortiz: Conceptualization, Supervision, Writing - Review & Editing

Declaration of interests

☒ The authors declare that they have no known competing financial interests or personal relationships that could have appeared to influence the work reported in this paper.

☐The authors declare the following financial interests/personal relationships which may be considered as potential competing interests: